ACS OMEGA

http://pubs.acs.org/journal/acsodf

Article

Physicochemical Profiling and Comparison of Research Antiplasmodials and Advanced Stage Antimalarials with Oral Drugs

Amritansh Bhanot and Sandeep Sundriyal*

Cite This: *ACS Omega* 2021, 6, 6424−6437

Read Online

ACCESS | Metrics & More | Article Recommendations | Supporting Information

ABSTRACT: To understand the property space of antimalarials, we collated a large dataset of research antiplasmodial (RAP) molecules with known *in vitro* potencies and advanced stage antimalarials (ASAMs) with established oral bioavailability. While RAP molecules are "non-druglike", ASAM molecules display properties closer to Lipinski's and Veber's thresholds. Comparison within the different potency groups of RAP molecules indicates that the *in vitro* potency is positively correlated to the molecular weight, the calculated octanol−water partition coefficient (clog *P*), aromatic ring counts (#Ar), and hydrogen bond acceptors. Despite both categories being bioavailable, the ASAM molecules are relatively larger and more lipophilic, have a lower polar surface area, and possess a higher count of heteroaromatic rings than oral drugs. Also, antimalarials are found to have a higher proportion of aromatic (#ArN) and basic nitrogen (#BaN) counts, features implicitly used in the design of antimalarial molecules but not well studied hitherto. We also propose using descriptors scaled by the sum of #ArN and #BaN (SBAN) to define an antimalarial property space. Together, these results may have important applications in the identification and optimization of future antimalarials.

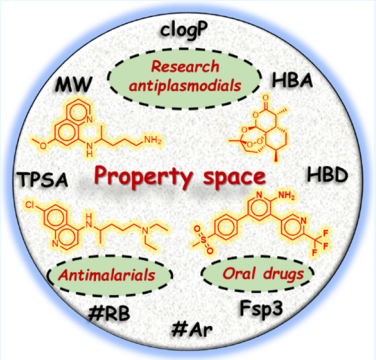

1. INTRODUCTION

Different studies have estimated costs between 2.8 and 9.8 billion dollars to bring a new drug to the market.[1,2] At the same time, the failure rate in the clinical studies remains high, that is attributable, inter alia, to poor bioavailability and safety.[3] Involvement of such high stakes in the drug discovery calls for diligent efforts in understanding the factors affecting "drug-likeness" or "druglike properties."

Although the specific definition of "druglikeness" is debatable,[4] broadly, it is akin to optimum oral bioavailability. The latter depends on the aqueous solubility, absorption, permeation, metabolic stability, and transporter-mediated efflux of a molecule, spawned by its interactions with several biomolecules and biomembranes *in vivo*. Thus, like the drug action, druglikeness is also a function of a molecule's chemical structure or physicochemical profile. Consequently, on average, orally available drugs represent an amalgamation of optimum physicochemical properties required to interact favorably with the human physiology.

One of the earliest attempts to understand the influence of molecular properties on druglikeness was undertaken by Lipinski *et al.* with the introduction of the rule of five (Ro5).[5] Lipinski's Ro5 proposes a cutoff for four molecular properties, namely, molecular weight (MW < 500 Da), calculated partition coefficient (clog P < 5), hydrogen bond acceptor (HBA < 10), and hydrogen bond donor (HBD < 5), to assess the druglike characteristics. Molecules within the recommended limits of at least two of these four descriptors are expected to have good permeation and absorption, resulting in good oral bioavailability. Despite several limitations[6] and criticisms,[4,7] the Ro5 still seems to be a useful criterion to eliminate non-ideal molecules in the early phase of drug discovery.[8,9] Since the seminal work by Lipinski, the role of other structural descriptors such as aromatic rings (#Ar),[10−12] the fraction of sp^3 carbon (Fsp^3),[13] topological polar surface area (TPSA),[14,15] distribution coefficient (log D),[16−18] and the number of rotatable bonds (#RB)[14] has also been recognized to affect the "developability" of a molecule. Some authors have proposed using score-based and other quantitative druglikeness metrics instead of the rules with hard cutoffs.[17,19] Additionally, mapping of compound optimization trajectories primarily based on the ligand efficiency and ligand lipophilic efficiency has also been recommended for successful drug hunting.[20−22]

Overall properties of drugs are also ought to be governed by the nature of their target. Indeed, drugs targeting different protein classes (such as kinases, nuclear hormone receptors, and proteases) possess variable properties.[20,23] This is because of these targets' distinct binding pockets requiring unique molecular size ranges, lipophilicity, ionization, or H-bonding

Received: January 7, 2021
Accepted: February 18, 2021
Published: February 25, 2021

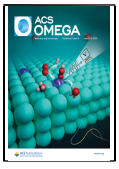

https://dx.doi.org/10.1021/acsomega.1c00104
ACS Omega 2021, 6, 6424−6437

capacity. For instance, compared to marketed oral drugs, orally available anticancer protein kinase inhibitors are larger, more lipophilic, and more complex.[24] Similarly, orally used anti-infective drugs have higher MW, low lipophilicity, and greater HBA/HBD and ring counts.[25−27] Specific properties may also be required to access a particular tissue/organ/organelle where a biological target might be residing, exemplified by the drugs acting on the central nervous system (CNS). In general, CNS drugs are smaller, lipophilic, and unionized than other drugs as there is a need for these molecules to overcome the blood−brain barrier.[28,29] Thus, a target- or organ-specific chemical space exists within a broad oral drug space. Optimal properties required by a molecule to interact with its biological target (for *in vitro* potency) may or may not be orthogonal to those required for desirable oral bioavailability. Therefore, understanding oral drug space in a particular biological target context may provide useful insights that guide the drug design for the given target/biological endpoint.

Malaria is an infectious disease caused by the *Plasmodium* species belonging to the Apicomplexan phylum, spread by the mosquito bite. Malaria mostly affects tropical and sub-tropical populations, with children and pregnant women being the most vulnerable groups.[30] Owing to the spread of resistant strains of the parasite, treatment of malaria involves a multi-drug regimen. In this context, the artemisinin combination therapy is regarded as a "gold standard," and it is used as the first-line therapy in malaria treatment. However, resistance is spreading against artemisinin at alarming levels[31−35] and may lead to devastating outcomes.[36] These concerns have prompted large-scale high throughput screening (HTS) campaigns against *Plasmodium falciparum,* resulting in a large amount of data for retrospective learning and prospective predictions. These efforts are mostly based on phenotypic whole-cell assays against asexual or sexual stages of the parasite and have produced novel leads and clinical candidates.[37−39] Despite the tremendous efforts in the past decade,[40] only two small antimalarial molecules, tafenoquine and arterolane, have been approved in the past 20 years.

The antiplasmodial molecules act through different targets residing in different organelles such as parasite cell membranes, mitochondria, apicoplasts, food vacuoles, and the cytoplasm. Since the parasite inhabits host red blood cells (RBCs), the molecules active in antiplasmodial phenotypic assays must cross at least three membrane barriers. The latter consists of the host RBC membrane, parasitophorous vacuolar membrane (PVM), and parasite plasma membrane.[41,42] Such a permeability barrier may impose specific properties to the active set of molecules compared to the inactive ones in these assays. For instance, large-scale phenotypic HTS by GlaxoSmithKline (GSK) found hit molecules to be larger and more lipophilic compared to the average source compound collection.[43] Thus, it would be interesting to perform a systematic analysis of the property space of research antiplasmodial (RAP) molecules with differential potencies. Such comparison may reveal the key chemical descriptors important for allowing permeation across host/parasite lipoidal membranes or target engagement. However, cellular permeation alone is not enough to achieve optimum oral bioavailability properties. Also, research molecules are known to differ from clinical candidates and drugs in terms of physicochemical properties.[21,44,45] Therefore, a comparison is required between RAP and the advanced stage antimalarial (ASAM) molecules with the proven *in vivo* oral bioavailability and efficacy. Such a comparison among RAP and ASAM would help map the trajectory as initial antimalarial hit advances from the discovery stage to the lead stage.[20] To further characterize the antimalarial property space, comparison with other oral drugs is also required.

We collated and studied the average properties of the above-stated datasets. The results reveal interesting differences and similarities in RAPs, ASAMs, and oral drugs in the property space. Furthermore, we have characterized an antimalarial property space that may facilitate the identification of new antimalarial molecules.

2. RESULTS AND DISCUSSION

2.1. Data Collection and Data Analysis. We used readily available open-source tools and resources for the data collection and the analysis. The set of RAP molecules was collated from the ChEMBL database, one of the largest collections of biologically active compounds reported in the medicinal chemistry literature.[46,47] Additionally, the results of several phenotypic HTS campaigns against *P. falciparum* have also been deposited in ChEMBL by pharmaceutical companies like GSK.[43] While compounds disclosed from such large screens may not be ideal for further development,[48] such data may be used for the physicochemical profiling of antimalarials. Nevertheless, to ensure the quality of activity data, we have included compounds tested at multiple concentrations against the parasite with known IC_{50}/EC_{50} values. Although several of these molecules are tested in different labs under different assay conditions, such heterogeneous data are acceptable for the qualitative comparison of bioactivities.[49] These molecules were classified into different potency classes (HA, MA, and IN, see Methodology) to observe the effect of various properties on the *in vitro* potency. The HA dataset is the largest one since mostly successful results are reported in the literature. Due to the same reason, the IN class was found to have comparatively few molecules, and hence, the latter was topped up with the inactive molecules reported by GSK-Tres Cantos Antimalarial Set (TCAMS) screening (see Methodology).[43]

In addition to the marketed antimalarials, the ASAM set consists of antimalarials currently undergoing clinical trials and molecules considered "leads" with promising efficacy and oral bioavailability in animal studies.[37,38] Thus, the difference between the RAP and ASAM molecular properties may indicate the influence these properties have on the "developability" of antimalarials.

For this study, the "oral drug" is defined as a small molecule (MW < 900 Da) currently approved by a regulatory body for oral administration to treat or prevent any disease in humans. The set of oral drugs was obtained from the DrugCentral[50] database, which consists of drugs approved not only by the US FDA but also by the regulatory agencies in Europe, Japan, and other countries. The library was further updated with the recently approved drugs by the US FDA (till July 2020). Consequently, our library of oral drugs is extended (total 1954) in comparison to the recently compiled set of 750 oral drugs used for property profiling.[4,8] The latter is limited to the oral drugs approved till 2017 by the US FDA.

While Lipinski suggested the cutoff of 500 Da for the MW, some authors have suggested that the actual limit for the MW may be higher for the orally absorbed drugs,[27,51,52] prompting us to use a cutoff of 900 Da for the collation of all datasets. Using these criteria, the final datasets of IN, MA, HA, ASAM, and oral drugs consist of 7365, 6620, 10,557, 66, and 1954 molecules, respectively. Some of the molecules are present in

https://dx.doi.org/10.1021/acsomega.1c00104
ACS Omega 2021, 6, 6424−6437

Table 1. Comparison of 90th and 10th Percentiles of Various Molecular Properties[a]

molecular property	oral drugs (N = 1954)	ASAM (N = 66)	HA (N = 10,557)	MA (N = 6620)	IN (N = 7365)
MW	519.0 (204.2),[b] 552.2 (197.0),[c] 470.3 (171.2)	500.9 (253.6)	588.8 (296.6)	568.7 (277.8)	567.1 (242.4)
clog P[d]	4.85 (−0.87),[b] 4.80 (−0.36),[c] 4.65 (−0.64)	5.54 (0.34)	6.43 (1.50)	5.78 (1.50)	5.64 (0.20)
HBA	9 (2),[b] 10 (2),[c] 10 (2)	8 (3)	9 (3)	9 (3)	10 (3)
HBD	4 (0),[b] 4 (0),[c] 4 (0)	4 (0)	4 (0)	3 (0)	4 (0)
TPSA	145.1 (27.4),[b] 143.3 (29.0),[c] 139.8 (21.3)	118.3 (43.2)	125.0 (33.1)	129.1 (33.5)	142.3 (34.9)
#Ar	3 (0),[b] 3 (0),[c] 3 (0)	4 (0)	4 (1)	4 (1)	4 (0)
#RB	10 (1),[b] 11 (1),[c] 10 (1)	9 (1)	12 (2)	11 (2)	12 (1)
Fsp^3	0.78 (0.13),[b] 0.78 (0.13),[c] 0.83 (0.08)	0.94 (0.12)	0.71 (0.09)	0.59 (0.07)	0.87 (0.07)

[a]The values in brackets represent 10th percentiles. [b]The 90th percentile values of all oral drugs (N = 750) approved by the US FDA for the period 1900−2017. Taken from the Supporting Information of ref 4. [c]The 90th percentile values for oral drugs (N = 341) approved before the proposal of the Ro5, that is, for the period 1900−1997. Taken from the Supporting Information of ref 4. [d]clog P values were calculated using the DataWarrior program for our dataset, while the StarDrop program was used in ref 4.

Table 2. Comparison of Mean/Median of Molecular Properties among the Different Categories of Molecules

	oral drugs (N = 1954)	ASAM (N = 66)	HA (N = 10,557)	MA (N = 6620)	IN (N = 7365)
molecular property	mean (median)	mean (median)	mean (median)	mean (median)	mean (median)
MW	357.2 (339.5)	389.9 (391.4)	432.2 (418.4)	408.8 (393.5)	384.0 (361.4)
clog P	2.23 (2.43)	3.07 (3.13)	3.94 (3.40)	3.60 (3.60)	2.90 (3.00)
HBA	5.48 (5)	5.60 (5.5)	5.80 (6)	5.68 (5)	5.82 (5)
HBD	1.90 (2)	2.10 (2)	1.70 (1)	1.52 (1)	1.85 (1)
TPSA	80.38 (72.34)	75.90 (73.11)	74.68 (69.30)	77.44 (71.44)	82.00 (73.12)
#Ar	1.70 (2)	2.12 (2)	2.73 (3)	2.65 (3)	1.97 (2)
#CarboAr	1.13 (1)	1.23 (1)	1.76 (2)	1.78 (2)	1.38 (1)
#HetAr	0.52 (0)	0.89 (1)	0.96 (1)	0.86 (1)	0.59 (0)
#RB	5.09 (4)	4.72 (4)	6.59 (6)	5.94 (5)	5.86 (5)
Fsp^3	0.432 (0.4)	0.423 (0.375)	0.355 (0.310)	0.314 (0.285)	0.407 (0.363)
#BaN	0.62 (1)	1.09 (1)	1.01 (1)	0.66 (0)	0.71 (0)
#ArN	0.60 (0)	1.16 (1)	1.10 (1)	1.03 (0)	0.75 (0)

more than one category. For example, several oral drugs are also part of the IN dataset. Similarly, currently marketed antimalarials are part of both ASAM as well as oral drug datasets.

The open-source program RDKit was used to calculate the MW, HBA, HBD, Fsp^3, #RB, #Ar, and heteroaromatic ring count (#HetAr), while DataWarrior was used for the computation of the clog P, TPSA, carboaromatic ring count (#CarboAr), aromatic nitrogen count (#ArN), and basic nitrogen count (#BaN). Comparison among the different categories of molecules was performed using various statistical parameters and hypothesis tests employed earlier in similar studies.[4,5,10,14] Given the skewness and kurtosis in the data (see Supporting Information), the Kruskal−Wallis test was employed for hypothesis testing, in addition to the t-test.[4] Certain properties like clog P, HBA, HBD, and TPSA are known to be correlated with the MW.[14] Hence, property trends were monitored for both large (MW > 500 Da) and small (MW < 500 Da) molecules within the given category (Supporting Information, Figures S3−S13). Expectedly, most of the molecules (∼80%) in our complete dataset belong to the latter class (Supporting Information, Table S2). The large molecules in the ASAM class possess only eight molecules, and hence, the results for this category should be interpreted with caution.

2.2. Comparison of the Globally Approved Oral Drugs with the FDA-Approved Drugs. Since our library consists of globally approved oral drugs, we compared it with the recently reported set of FDA-approved oral drugs. Most of the physicochemical properties can be computed unambiguously except for log P, which displays variable results based on the algorithm and computational programs used.[4] For this study, we used the open-source Actelion clog P algorithm implemented in the DataWarrior program,[53] which recognizes 368 atom types contributing toward the final value. This algorithm has been shown to outperform many other programs when tested on a dataset of 96,000 compounds.[54] Moreover, a satisfactory correlation was observed for Actelion clog P versus the experimental log P (0.882) and Actelion clog P versus StarDrop clog P (0.935) (Supporting Information, Figures S1 and S2) for the set of 452 drugs compiled by Shultz.[4]

Despite the different compilation criteria and clog P algorithms, our extended set and the FDA-approved oral drugs show comparable 90th and 10th percentile values for important physicochemical properties (Table 1). The 90th percentiles for all properties, except for MW, are within Lipinski's cutoffs for both the libraries. Consequently, 786 out of 1954 drugs (∼91%) in our library pass the Ro5. The drop in the 90th percentile of MW in our dataset (519.0 Da) in comparison to that of the FDA drugs (552.2 Da) may be due to the applied MW cutoff of 900 Da in the former case. Moreover, 90th percentiles of the TPSA and #RB of both libraries are also close to the limits proposed by Veber *et al.* for optimum bioavailability.[14] The 90th and 10th percentiles for #Ar and Fsp^3 descriptors are also identical for both libraries. The comparison of FDA-approved oral drugs before 1997[4] with the combined oral drugs demonstrates slight inflation in MW, clog P, and TPSA descriptors, in line with the earlier reports.[4,21,25]

https://dx.doi.org/10.1021/acsomega.1c00104
ACS Omega 2021, 6, 6424−6437

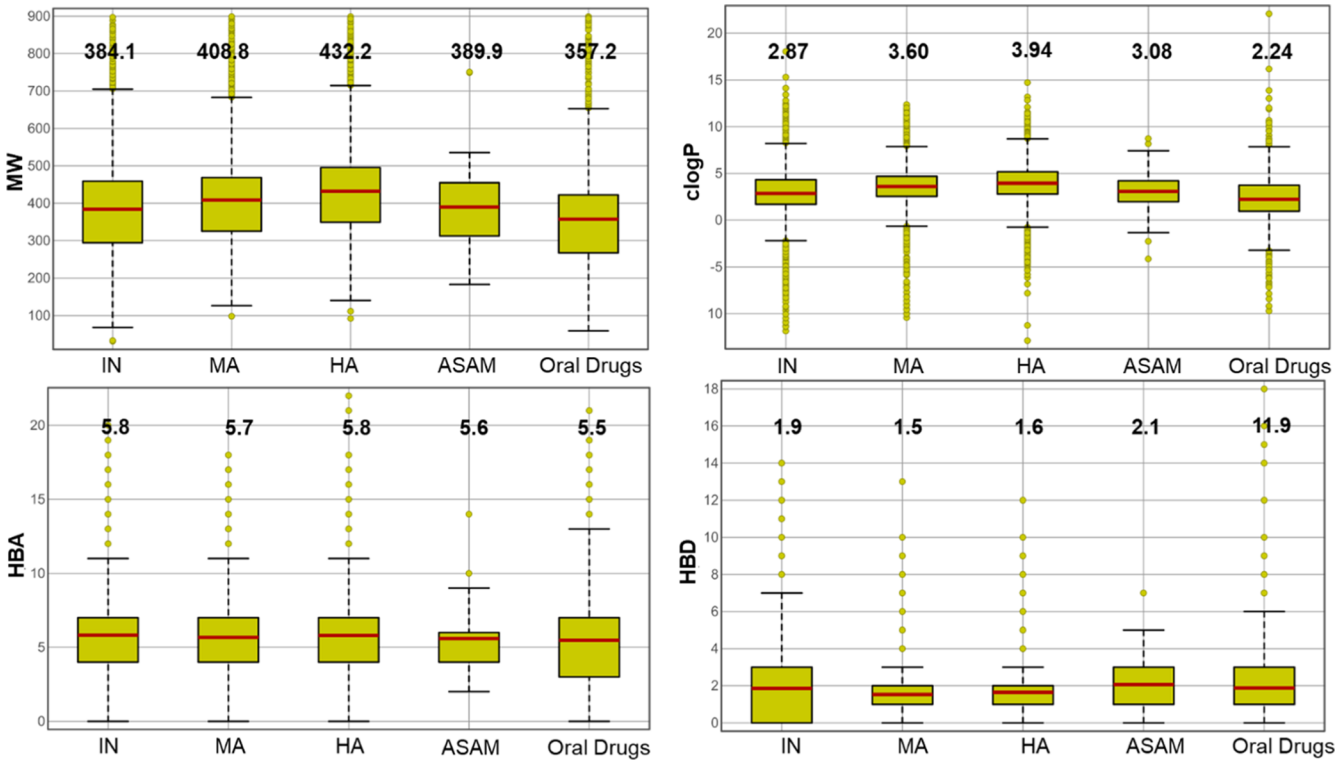

Figure 1. Boxplots for the MW, clog *P*, HBA, and HBD properties for different sets of molecules. The mean values are given in bold above each boxplot and represented by the red line within the boxes. The yellow dots represent outliers.

For charged molecules, log *D* may be more relevant than clog *P* as a measure of lipophilicity. This is evident from the application of the property forecast index and AbbVie multiparametric scoring function in judging compound quality.[16−18] However, our analysis is limited to clog *P* and other key properties as we do not have access to any commercial software for log *D* calculation. Also, to our knowledge, no open-source program is available to compute log *D* for an extensive database such as the one used in this study.

Overall, our oral drug library is updated with the most recent approvals and conforms to the property space of druglike compounds reported by other authors.

2.3. MW and clog *P*. MW has been shown to affect oral absorption, especially of hydrophilic drugs. The latter are mostly absorbed through paracellular spaces or cell junctions, which have a restricted size of 3−6 Å in humans. This is supported by the distinctive absorption kinetics of polar drugs observed in different species of animals and is attributable to the variation in the paracellular pore size.[55] Nevertheless, Lipinski's cutoff of MW may also arise from the limited number of large molecules pursued in drug discovery due to the challenges associated with their synthesis[4,56] or due to the limit imposed by other descriptors correlated to MW.[14,57] Lipophilicity affects the cellular uptake and oral absorption by influencing dissolution and partitioning of a drug into the lipid bilayer.

In RAP molecules, the mean (and median) MW increases with increasing antiplasmodial activity (Table 2, Figure 1). The HA and MA categories display significantly higher MW than the IN class. This trend is also visible in 90th and 10th percentile values for MW for these classes. The average MW of the ASAM group is lower (389.9 Da) compared to that of the HA class (432.1 Da) but higher than that of the oral drugs (357.2 Da), results statistically significant according to the *t*-test but not the Kruskal−Wallis test. The 90th percentile for the MW of the ASAM molecules (500.9 Da) is almost identical to the threshold of 500 Da suggested by Lipinski.

Like MW, mean and 90th percentile values for clog *P* also show a steady increase from IN to MA to HA categories (Figure 1), suggesting a positive correlation between lipophilicity and antiplasmodial activity in phenotypic assays. However, like MW, the clog *P* of ASAM molecules also converges back to lower values while maintaining a statistically higher average than that of the oral drugs, as per the *t*-test. The trend is maintained for both low and high MW categories of RAP molecules, with average clog *P* showing an increase with increasing potency (Supporting Information, Figure S3).

In summary, bulkier and lipophilic molecules tend to show potent *in vitro* antiplasmodial activity, which agrees with GSK-TCAMS screening results.[43] This means that in the currently used antiplasmodial phenotypic assays, membrane permeability of molecules is not adversely affected by their large size or high lipophilicity. Nevertheless, to advance these molecules in the antimalarial pipeline, MW and clog *P* must be optimized toward Lipinski's thresholds.

RAP molecules' high permeability despite their bulky and lipophilic nature may result from their facilitated transport *via* parasite-induced new permeation pathways. The latter allows the entry of diverse molecules within the infected RBC.[58] For instance, the plasmodial surface anion channel linked to the *clag* gene family[59] induced on the infected RBC membrane can carry large and lipophilic molecules.[60] Once inside the infected RBCs, these molecules may further cross the PVM, which itself contains several non-selective channels to carry bulky molecules.[61−63] The high lipophilicity may also allow molecules to partition within the lipid portion of the biological

https://dx.doi.org/10.1021/acsomega.1c00104
ACS Omega 2021, 6, 6424−6437

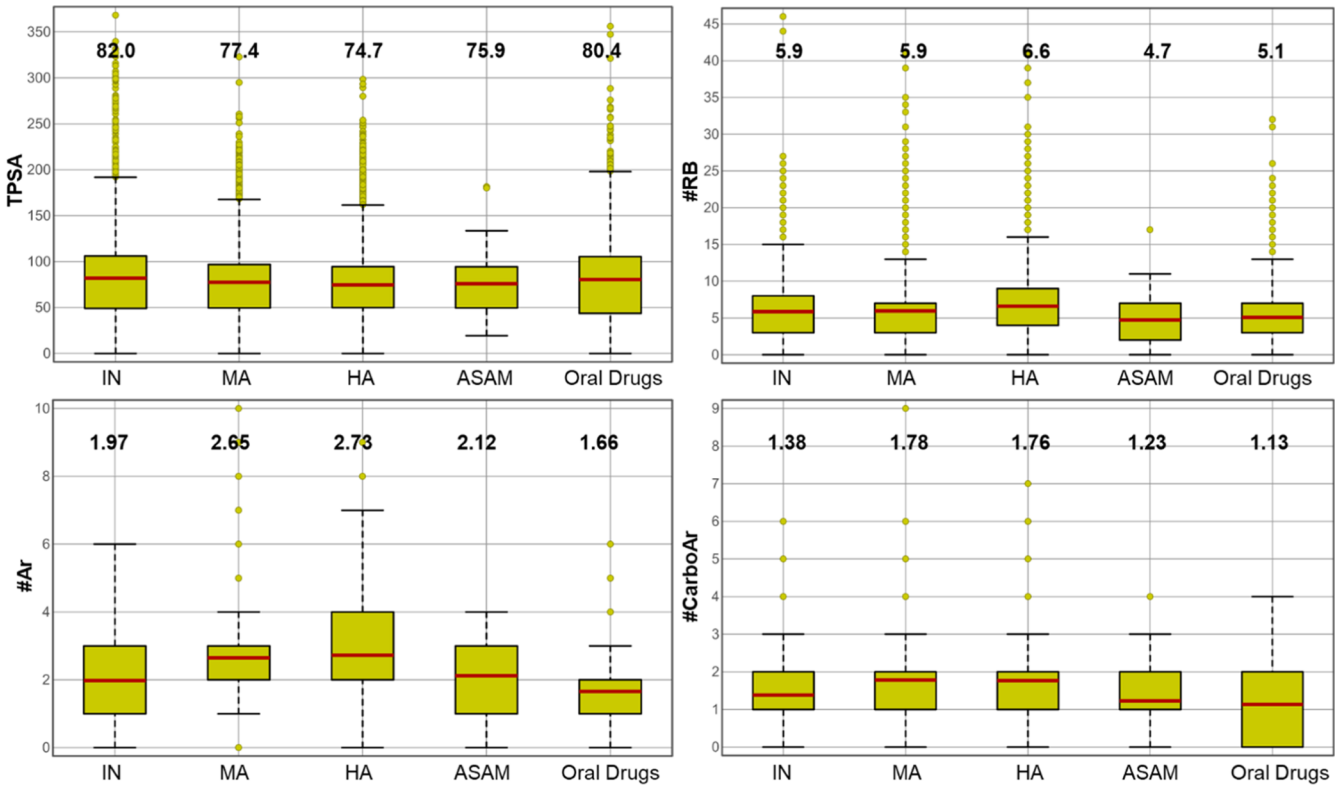

Figure 2. Boxplots for the TPSA, #RB, #Ar, and #CarboAr properties for different sets of molecules. The mean values are given in bold above each boxplot and represented by the red line within the boxes. The yellow dots represent outliers.

membrane, thus enabling passive diffusion.[64] However, such "obese"[65] molecules are likely to exhibit low solubility, extensive metabolism, and P-glycoproteins-mediated efflux, preventing their progression to the ASAM category, which explains the relatively lower MW and clog *P* averages of the latter class.

2.4. HBA and HBD. The HBA (sum of O and N atoms) and HBD (sum of NH and OH groups) are important parameters that determine the overall polarity and H-bonding capacity of a molecule. These two descriptors also affect the aqueous solubility,[66,67] a prerequisite for oral absorption.

The HA and MA molecules show a significantly higher average HBA but lower HBD compared to the oral drugs (Table 2, Figure 1). The ASAM molecules display averages for HBA and HBD that do not differ statistically to those of oral drugs. However, the 90th percentile for both descriptors complies with Lipinski's thresholds for all the categories of molecules. The larger antimalarial molecules (MW > 500 Da) consistently display lower HBA and HBD than the oral drugs, and the averages decrease with increasing *in vitro* potency. Overall, for small molecules (MW < 500), the HBA and HBD do not seem to have a noticeable influence on the antimalarial activity, but lower values for these descriptors are preferred for larger molecules.

2.5. TPSA and #RB. Veber and co-workers demonstrated TPSA and #RB descriptors to be the better predictors of oral bioavailability in comparison to the Ro5 with their undisclosed dataset (N = 1100).[14] The molecules with a TPSA ≤ 140 Å^2 and #RB ≤ 10 were found to have good oral bioavailability in rat models. In DataWarrior, TPSA is calculated using the original approach of Ertl *et al.*, which was also adopted by Veber and co-workers.[68] Our dataset of oral drugs (N = 1954) displays comparable results with the 90th percentiles of 144.7 Å^2 and 10 for the TPSA and #RB, respectively (Table 1).

In RAP molecules, mean TPSA decreases (Figure 2) with an increase in potency (IN = 81.99 Å^2, MA = 77.44 Å^2, and HA = 74.68 Å^2), with 90th percentiles also showing the same trend (Table 1). While the HA and MA molecule averages are significantly lower than that of the oral drugs (as per the *t*-test but not the Kruskal–Wallis test), statistical difference is not observed either between the HA/MA versus ASAM (75.9 Å^2) or ASAM versus oral drugs (80.4 Å^2). Interestingly, ASAM molecules display the lowest 90th percentile (mean = 118.3 Å^2) among all categories. This trend of TPSA variation is exhibited by small and large molecules, albeit differences are more dramatic in the latter case (Supporting Information, Figure S6). Inclusively, these results suggest that a lower TPSA is advantageous for both *in vitro* and *in vivo* antimalarial activity, especially for the larger molecules. Presumably, higher polarity negatively affects permeability across the multiple membranes that an antimalarial molecule must cross.[41]

The average for the #RB descriptor increases (Figure 2) significantly with increasing antiplasmodial potency, especially for the smaller molecules (Supporting Information, Figure S7), with the HA class displaying the highest mean of 6.6. In contrast, the ASAM molecules are relatively rigid, with fewer #RB (mean = 4.7) comparable to that of the oral drugs (mean = 5.09), suggesting that high flexibility or a greater RB count is not detrimental to the *in vitro* antiplasmodial activity. Nevertheless, lower #RB averages of ASAMs and oral drugs as compared to that of the HA molecules confirms the importance of lower flexibility for overall oral bioavailability and agrees with the observation of Veber *et al.*[14]

https://dx.doi.org/10.1021/acsomega.1c00104
ACS Omega 2021, 6, 6424−6437

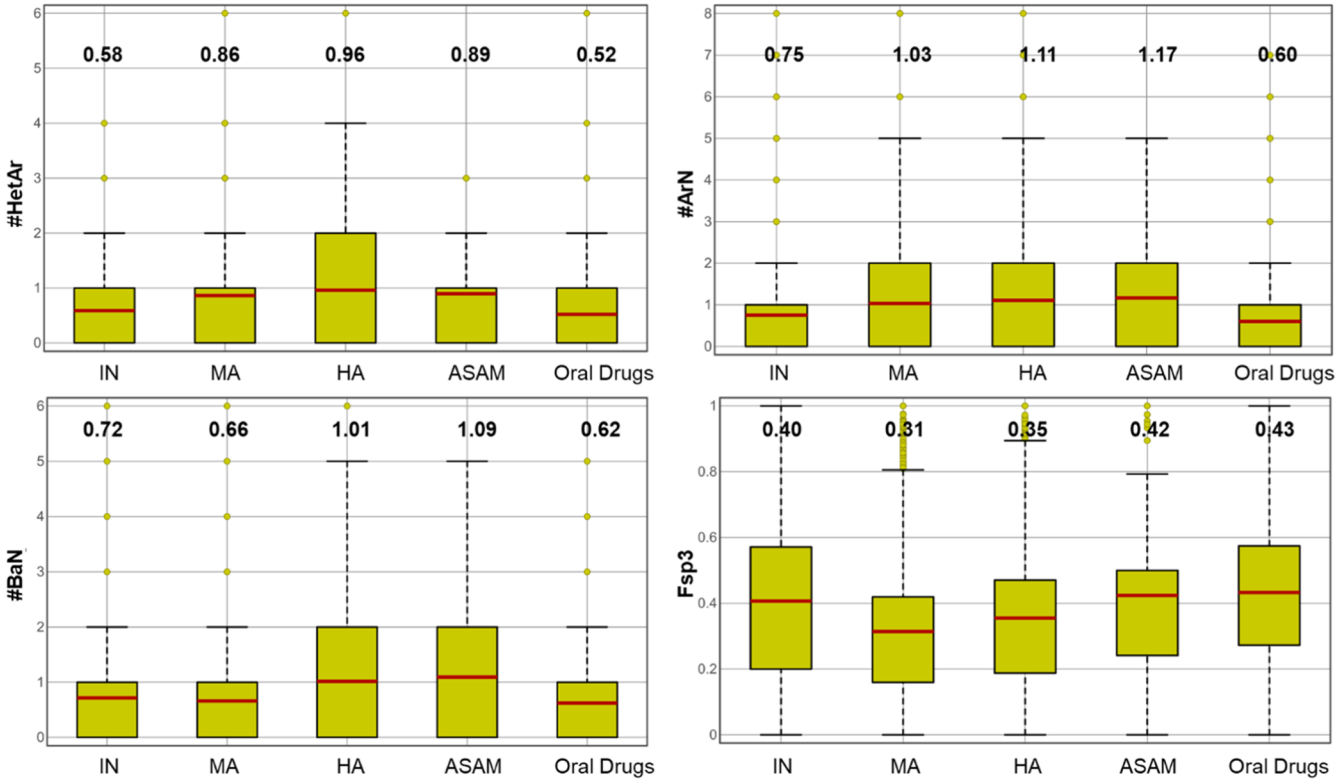

Figure 3. Boxplots for the #HetAr, #ArN, #BaN, and Fsp^3 properties for different sets of molecules. The mean values are given in bold above each boxplot and represented by the red line within the boxes. The yellow dots represent outliers.

2.6. #Ar and Type of Rings. The number and nature of rings in a molecule can influence a molecule's physicochemical properties, ultimately influencing its clinical success.[10−12] The high attrition rate of molecules with a higher #Ar may be due to the low water solubility, high protein binding, and non-specific binding with other proteins leading to undesired effects. One crucial implication of the high content of aromatic carbons is the inhibition of human ether-à-go-go-related gene (hERG) channels that may lead to cardiotoxicity.[10]

On average, the HA molecule possesses more aromatic rings (mean = 2.73) than the MA (mean = 2.65) and IN (mean = 1.97) categories (Figure 2). However, the mean #Ar falls significantly in ASAM molecules (mean = 2.12) compared to that of HA but is still greater than that of oral drugs (mean = 1.66). These results are statistically significant, as indicated by both the *t*-test and the Kruskal−Wallis test. The 90th percentile for #Ar in ASAM and RAP molecules is 4, a unit higher than that of the oral drugs. This trend for #Ar also seems to be equally important for the large and small molecules (Supporting Information, Figure S8), suggesting aromaticity to be a key determinant for both *in vitro* and *in vivo* antimalarial activity.

The structurally related carboaromatic and heteroaromatic rings (*e.g.*, phenyl *vs* pyridine) display distinct values of lipophilicity, polarity, conformation preference, and H-bond capability.[69] Consequently, the carboaromatic ring count (#CarboAr) and heteroaromatic ring count (#HetAr) descriptors have varying influences on a molecule's pharmacokinetics and pharmacodynamic profile.[12]

While the mean #CarboAr of the ASAM category (1.23) is not different from that of the oral drugs (1.13), the #HetAr mean of bioavailable ASAMs (0.89) is significantly higher as compared to the mean of oral drugs (0.52). Additionally, for active molecules (HA and MA), both #CarboAr and #HetAr are significantly higher than those of the IN class. A similar trend is observed in both the high and low MW class of compounds (Supporting Information, Figures S9 and S10). These observations suggest that while aromaticity is vital for both *in vitro* and *in vivo* antimalarial activity, there is a need to limit the #CarboAr to advance the antimalarial molecules toward clinical application. These observations agree with an earlier study, which suggests that a higher #CarboAr has a more substantial detrimental effect on a compound's developability than a higher #HetAr.[12]

Given the importance of nitrogen-containing heterocycles in drug discovery,[70] in general and for antimalarial drug discovery,[71−73] in particular, we analyzed the aromatic nitrogen count (#ArN) in all compounds.

The #ArN is positively correlated with *in vitro* potency, as apparent from the mean #ArN for HA (1.11), MA (1.03), and IN (0.75) categories (Figure 3). The ASAM molecules display a mean value of 1.17 for the #ArN, which is significantly higher than that of the oral drugs (0.60) but not that of the HA class. However, the #ArN seems to be more critical for low MW compounds than for the bulkier molecules (Supporting Information, Figure S11). All antimalarial categories also display the 90th percentile of 3 for the #ArN, one unit higher than that of the oral drugs. The proportion of molecules possessing at least one N-heteroaromatic ring also increases with an increase *in vitro* antiplasmodial activity (HA > MA > IN) and attains the highest value of ∼62% for ASAM molecules (Supporting Information, Table S2), much higher than that of the oral drugs (∼30%). In contrast, no noticeable trend was observed for the aliphatic N-heterocycle, with all molecules showing similar percentages (Supporting Information, Table S2). Amongst all aromatic N-heterocycles, the

https://dx.doi.org/10.1021/acsomega.1c00104
ACS Omega 2021, 6, 6424−6437

Table 3. Number of Molecules Compliant to the Specified Guidelines

guidelines	oral drugs (N = 1954)	ASAM (N = 66)	HA (N = 10,557)	MA (N = 6620)	IN (N = 7365)
Lipinski's Ro5	1786 (91%)	59 (89%)	8713 (83%)	5777 (87%)	6451 (88%)
Veber's rule	1647 (84%)	61 (92%)	8693 (82%)	5609 (85%)	5933 (81%)
guideline-1 s-TPSA 5 to 65; s-RB ≤ 6; s-HBA ≤ 5; s-HBD ≤ 2	1338 (68%)	60 (91%)	8234 (78%)	4823 (73%)	4924 (67%)
guideline-2 s-TPSA 5 to 65; s-RB ≤ 6; s-HBA ≤ 5; s-HBD ≤ 2; MW ≥ 235	1114 (57%)	60 (91%)	8090 (77%)	4639 (70%)	4418 (60%)

quinoline ring appears most frequently in antimalarial molecules, followed by pyridine and pyrimidine (Supporting Information, Table S3). The latter two rings are also prevalent in oral drugs, an observation in line with the earlier reports.[11,74]

Together, these observations suggest that higher content of the #ArN is favorable for the *in vitro* and *in vivo* antimalarial activity, and N-heterocyclics have a high probability of advancing in the antimalarial discovery pipeline.

A high content of the #CarboAr and #HetAr in antimalarials may be attributed to the historical success of quinoline-based antimalarials. The quinoline ring consists of two aromatic rings, one CarboAr and one HetAr. After several years, quinoline derivatives are still being pursued as antimalarials due to the synthetic tractability, cost-effectiveness, and ability of quinoline-based molecules to retain activity against chloroquine-resistant *Plasmodium* strains.[75] Consequently, the antimalarial literature is replete with quinoline and related heterocyclic molecules.[71] Additionally, several hybrid molecules[76,77] and bisquinoline molecules[78−81] are reported to possess potent antiplasmodial activity. The former consists of 4-aminoquinoline pharmacophore in conjunction with other heterocycles, while the latter contains two quinoline rings (total four #Ar) attached with a variable linker. Such bulky molecules are represented more in the RAP molecules, resulting in a higher #Ar and a high MW in these sets of molecules (*vide supra*).

Most of the quinoline and related N-heterocycle-based antimalarials target the hemozoin formation inside the parasite food vacuole. The latter is an essential process carried by the parasite to detoxify heme resulting from the hemoglobin degradation.[82−85] The quinoline and related cyclic scaffolds foster π-stacking interactions with the porphyrin's pyrrole rings, thereby inhibiting the nucleation and growth of the hemozoin crystals.[84,86−89]

In the context of target engagement, aromatic nitrogen can also act as an HBA and may dramatically improve potency, as observed for *Plasmodium* L-lactate transporter (PfFNT) inhibitors.[90] Another reason for the prevalence of N-heteroaromatics in the antimalarial design might be the emergence of *Plasmodium* kinases as drug targets.[91−93] The majority of kinase inhibitors target the adenosine triphosphate (ATP)-binding pocket of the kinases, and several N-heterocycles mimic the adenosine ring of ATP. Another speculation may be that flatness might be favorable for transporting these molecules across the RBC or parasite membranes mediated by hitherto undiscovered transporters.

2.7. Fraction of sp^3 Carbons (Fsp^3). The fraction of sp^3 hybridized or tetrahedral carbons (Fsp^3), calculated as the ratio of sp^3 carbons to total carbons, is another critical physicochemical descriptor.[13] The oral drugs are known to attain a higher Fsp^3 in comparison to the clinical candidates. The higher Fsp^3 correlates well with improved solubility and lower melting points, factors likely to improve oral bioavailability.[13,94,95] This observation is confirmed with our compiled library of oral drugs and ASAM molecules, both of which possess higher 90th percentile values and averages for Fsp^3 than that of RAP molecules (Tables 1 and 2). The Fsp^3 and #Ar descriptors show an overall negative correlation (r = −0.632 for all molecules), yet the ASAM molecules possessing a higher 90th percentile for the #Ar also display a higher 90th percentile for the Fsp^3, in comparison to that of the oral drugs. Among RAP molecules, MA and HA categories possess a significantly lower Fsp^3 (Figure 3) than the ASAM/oral drugs categories; a trend also observed in both small and bulkier molecules (Supporting Information, Figure S12). Together with the #Ar (*vide supra*), the results of Fsp^3 analysis reemphasizes that the flat structure of antimalarials may have a positive influence on the *in vitro* potency. Nonetheless, as suggested for other orally available drugs,[13] a higher Fsp^3 is advantageous to advance antimalarials in the drug discovery pipeline.

2.8. Basicity. In DataWarrior, the basic nitrogen count (#BaN) can be used to estimate the molecule's basicity. The #BaN descriptor is based on a set of empirical rules rather than the computation of pK_a values. In addition to the amine groups, nitrogen atoms in certain heterocycles, such as quinoline, pyridine, and imidazole, are counted as BaN depending on the other ring substituents. However, only a weak correlation (0.328) is observed between the #BaN and #ArN in the dataset, suggesting the two descriptors to be orthogonal.

On average, all categories of antimalarial molecules possess a higher #BaN (Figure 3); however, statistical significance is displayed only in the case of oral drugs versus ASAM and oral drugs versus HA categories. Among RAP molecules, HA molecules possess a significantly higher #BaN than MA and IN molecules. These trends are also found to apply to small and large molecules (Supporting Information, Figure S13). Also, #BaN 90th percentiles are consistently higher for all antimalarials than that of oral drugs. This observation confirms the importance of basic character for antimalarial molecules for *in vitro* as well as *in vivo* activity.

The presence of basic centers in the form of amines or ArN (as in aminoquinolines) is known to improve the *in vitro* antiplasmodial potency of molecules acting through diverse mechanisms.[96−102] This is especially true for the antimalarials that target hemozoin formation within the parasite digestive vacuole (DV).[84,103−105] The basic molecules ionize inside the acidic contents of the parasite's DV[106] leading to their entrapment and high intravacuolar concentration.[104,106] The basic side chain and ring nitrogen of quinoline antimalarials are also proposed to make crucial interaction with the heme.[84,98,102,107] In fact, the initial ionic interaction between the protonated nitrogen of the chloroquine side chain and heme carboxylate may be required to bring these together for further binding.[107] The slightly lower cytoplasmic pH of the parasite[105] might also be the driving force for the internalization of the basic molecules.[105] In summary, the basicity of

https://dx.doi.org/10.1021/acsomega.1c00104
ACS Omega 2021, 6, 6424−6437

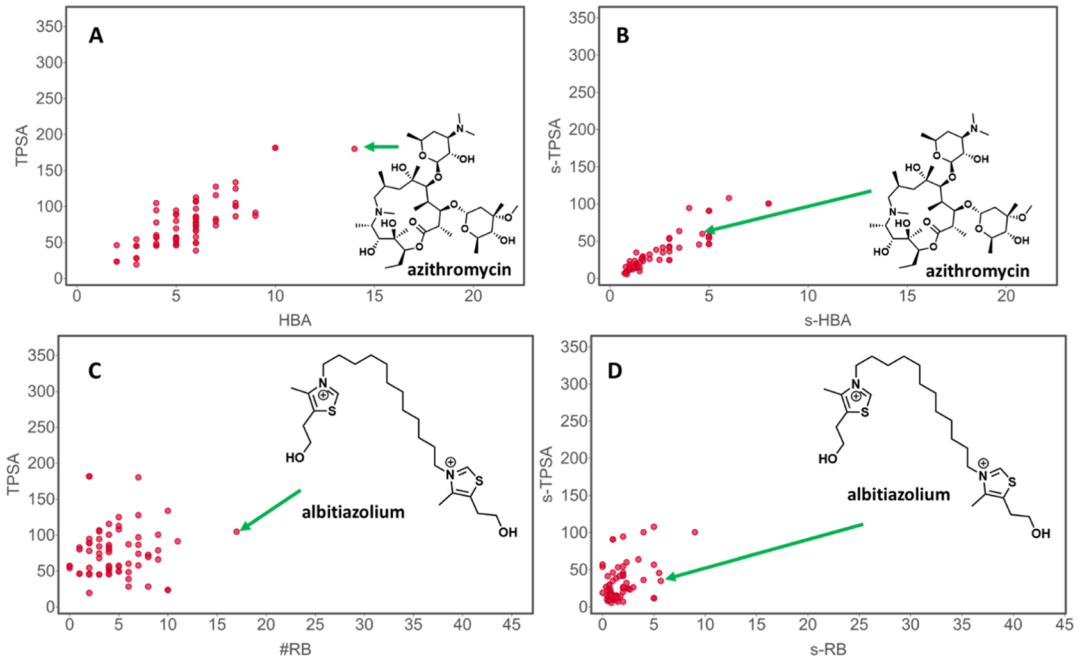

Figure 4. Plots showing ASAM molecules (red circles) in the property space. The bulky and polar azithromycin (A) converges to the antimalarial space defined by guideline-2 (B) when the corresponding scaled descriptors, s-TPSA and s-HBA, are used. Similarly, highly flexible and polar albitiazolium (C) also moves to the antimalarial space (D) following the application of the scaled descriptors, s-TPSA and s-RB.

antimalarials may be necessary for both target binding and distribution within the parasite and its acidic DV. Also, the basic nitrogen centers are often added during lead optimization to improve solubility and metabolism, resulting in improved bioavailability.[69,100] This justifies the highest proportion of the #BaN and #ArN in ASAM molecules compared to that of RAP molecules. One notable exception is the artemisinin class of antimalarials,[108] which lack ArN or BaN in their structure and yet possess high *in vitro* and *in vivo* potency.

2.9. Antimalarial Property Space. One of this study's objectives was to probe if an antimalarial space may be defined within the broad oral drug space. According to the widely cited Lipinski's and Veber's rules, the majority of the compounds in all categories conform to the drug-like space (Table 3). Expectedly, oral drugs and ASAM molecules show higher compliance for both rules. However, the combination of various fundamental properties used in these rules (MW, clog *P*, HBA, HBD, TPSA, and #RB) did not reveal a property space typical to that of antimalarial molecules. Given the importance of the #BaN and #ArN in antimalarials (*vide supra*), we hypothesized that these structural features might be used as a scaling factor to differentiate antimalarials from other molecules. Thus, a new descriptor, the sum of #BaN and #ArN (SBAN), was defined and used to scale various Lipinski's and Veber's properties by taking the latter's ratio to the factor of 1 + SBAN.

Interestingly, the property space described by the resulting scaled descriptors (s-MW, s-clog *P*, s-HBA, s-HBD, s-TPSA, and s-RB) revealed the confinement of the ASAM molecule to a narrow region within the broad druglike space. Two typical examples of azithromycin and albitiazolium are represented in Figure 4. Azithromycin is overtly bulky (MW 749 Da) and highly polar (TPSA 180 Å^2) due to several HBAs. However, the SBAN value of 2 in azithromycin results in lowered s-HBA and s-TPSA, pushing it to the antimalarial space with other ASAM molecules (Figure 4A *vs* 4B). Similarly, highly flexible albitiazolium (#RB = 17) also relocates to the antimalarial space upon using scaled descriptors (Figure 4C *vs* 4D).

These results encouraged us to propose guidelines or thresholds based on the scaled descriptors to characterize an antimalarial property space, particularly for the ASAM class. Based on the importance of individual properties and various plots between different scaled descriptors, we focused on s-TPSA, s-RB, s-HBA, and s-HBD. We found guideline-1 based on s-TPSA (5−65 Å^2), s-RB (≤6), s-HBA (≤5), and s-HBD (≤2) to be more selective for antimalarial molecules (ASAM, HA, and MA) than for other oral drugs and IN molecules. 91% of ASAM, 78% of HA, and 73% of MA molecules comply with guideline-1, while only 68% of oral drugs and 67% of IN class are included in the same region (Table 3; Figure 5). Adding a threshold of MW ≥ 235 Da (guideline-2) further resulted in improved selectivity for the ASAM compared to that of the

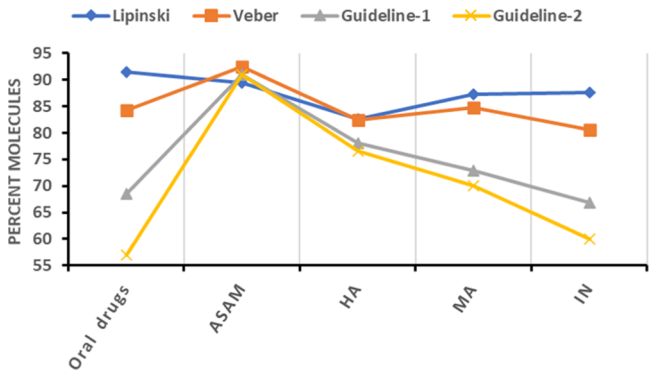

Figure 5. Plot portraying the percentage of molecules in compliance with specific guidelines. While most of the molecules in each category pass Lipinski's and Veber's rules, the thresholds based on the scaled descriptors (guideline-1 and guideline-2) are more selective for antimalarials.

https://dx.doi.org/10.1021/acsomega.1c00104
ACS Omega 2021, 6, 6424−6437

oral drugs and IN category. These results highlight the importance of the SBAN-scaled descriptors in defining the antimalarial drug space. Interestingly, all six ASAM molecules not complying with guideline-2 have high TPSA with no (or only one) SBAN count, resulting in their exclusion with the application of only the s-TPSA threshold (60−65 Å^2). Five of these are natural products (or natural product analogue) displaying high polarity owing to the presence of carboxylic (artesunate and CDRI 9778), phosphonic (fosmidomycin), or phenolic/enolic (tetracycline and doxycycline) acidic moieties (Supporting Information, Figure S14). The dapsone, on the other hand, possesses two aromatic amines that are not considered "basic" by the DataWarrior program.

Several oral drugs and their close analogues have been shown to have potent activity against *P. falciparum* in several repurposing studies.[109−113] As a result, out of the 1114 oral drugs picked by the guideline-2, 186 are already part of either RAP or ASAM libraries. Interestingly, of the remaining 928 oral drugs, 516 (∼56%) show the SkelSpheres[53] descriptors-based similarity of 0.7 or more to at least one HA or MA class of molecules. These observations further raise confidence in the use of guideline-2 for defining the antimalarial property space and offer a testable hypothesis. For example, it would be interesting to systematically evaluate these drugs, some of which are recently approved, against the parasite.

3. CONCLUSIONS

In summary, this work provides insights into the average property space of RAP and ASAM molecules, vis-à-vis oral drugs using readily available open-source cheminformatics tools. The RAP molecules are significantly "obese"[65,114] and belong to "flatland".[13] These research molecules display a positive correlation between their MW, #Ar, and clog *P* descriptors and *in vitro* potency (IN < MA < HA). However, for ASAM molecules, these properties converge close to Lipinski's Ro5 thresholds while still maintaining higher averages than those of oral drugs. This suggests that overtly higher MW, lipophilicity, and a flat molecular shape may be helpful for the permeability across the RBC/parasite membranes, but lower values are preferred to obtain clinical or lead antimalarials. These observations also highlight the inability of the whole-cell antiplasmodial assays to filter out non-ideal molecules, which is an often-cited advantage of phenotypic assays.

Although a higher #Ar seems to contribute to *in vitro* potency, druglikeness is maintained only by increasing the #HetAr rather than the #CarboAr.[11,12] Similarly, the higher average and 90th percentile of the Fsp^3 descriptor in the ASAM and oral drugs than that of RAP molecules reconfirm its influence on clinical success.[13] The HBA/HBD descriptors appear to be significant only for the bulky (MW > 500 Da) molecules with lower values favoring antimalarial activity. The lower TPSA and #RB also improve the likelihood of obtaining antimalarials with oral bioavailability, an observation in line with that of Veber *et al.*[14]

We also recognized that the #ArN and #BaN, the lesser-studied descriptors, are essential elements present in structurally diverse antimalarials, including historically successful aminoquinolines. Both the #ArN and #BaN might be assisting in target engagement and/or distribution within the parasite's acidic DV. We found a positive correlation between antimalarial activity and the #ArN and #BaN, while oral drugs were revealed to have lower values for these two descriptors. The high #ArN is primarily due to the expansive explorations of quinoline, pyridine, and pyrimidine rings, while amine groups contribute to the high #BaN. Judging by its high frequency in all categories of antimalarial molecules, the quinoline ring is still relevant to the antimalarial drug design.

We also propose the use of properties scaled by the SBAN count to define a region in the property space where the probability of finding druglike antimalarials (ASAMs) seems to be high. Two guidelines specifying the thresholds of scaled descriptors are suggested, albeit natural product-like molecules with acidic functionalities do not appear to conform to this space. In a physiological context, it seems that the SBAN count and other favorable properties assist antimalarials in crossing multiple membrane barriers to reach the intracellular targets of the parasite.[41] There is a clear indication that the *Plasmodium*'s highly evolved transportome[41,115−117] interacts with several marketed or advanced-stage antimalarials either as an antimalarial target or as part of a resistance mechanism.[115,117] Thus, a family of transporters in the parasitized RBC or PVM may be responsible for transporting antimalarials within the property space identified in this study. This is in line with Kell's hypothesis, implying that the carrier-mediated cellular uptake of molecules is more common than the diffusion across the phospholipid bilayer.[118−121] This is supported by the fact that the majority of drugs display high similarity to natural human metabolites.[122] It must be noted, however, that the characterization of *Plasmodium*'s transporters and their substrate specificities is challenging owing to its complex biology.

Overall, these results may have important implications in future explorations of antimalarial molecules. In general, relatively bulky, lipophilic, and flat molecules consisting of nitrogen scaffolds decorated with amine groups seem to be preferable candidates for antimalarial drug design. The libraries conforming to the proposed antimalarial property space may provide higher hit rates in experimental or virtual HTS studies.

Specific properties, such as MW, may change over time, apparently due to the exploration of newer targets and technologies.[4,21,25] This change may also be reflected upon antimalarial leads and drugs.[123] Hence, property-based studies such as this should be reassessed as more data emerge in the future.

4. METHODOLOGY

4.1. Data Curation. The ChEMBL-26 database[124] was searched within the DataWarrior program (version 5.2.1) to obtain the RAP set of molecules.[53] The molecules screened in a whole-cell phenotypic assay against "*P. falciparum*" were imported within DataWarrior where macromolecules (MW > 900 Da) and organometallic compounds were removed. The compounds annotated with definite IC_{50} or EC_{50} values (with the qualifier "=", "∼"; and not "<", ">") in nM or μM units were retained, and salt forms were neutralized. The canonical codes were generated using the DataWarrior program, and duplicate molecules were merged. In the case of multiple IC_{50}/EC_{50} values for the same compounds, the geometric average was calculated. The molecules with a large difference (>10 folds) in its multiple IC_{50}/EC_{50} values were discarded. The average IC_{50}/EC_{50} values were used for the classification of RAP molecules into "highly-active" (HA) ($IC_{50}/EC_{50} \leq 1000$ nM), "moderately active" (MA) (IC_{50}/EC_{50} 1001−9999 nM), and "inactive" (IN) ($IC_{50}/EC_{50} \geq 10{,}000$ nM) classes. The molecules found to be inactive in the HTS study conducted by

https://dx.doi.org/10.1021/acsomega.1c00104
ACS Omega 2021, 6, 6424−6437

GSK using the TCAMS[43] were also added to the IN set to expand the latter. The data for the TCAMS screening was downloaded from ChEMBL-neglected tropical disease webpage.[125] Only small (MW < 900 Da) and non-redundant molecules found to be inactive against both DD2 and 3D7 strains (for which no percentage inhibition data is reported) were retained (total 4351). The ASAM set of molecules was gathered from various literature reports (see Supporting Information, Table S1) and consisted of 33 marketed antimalarials, 19 clinical candidates, and 14 lead molecules. The structure of oral drugs was downloaded from DrugCentral[50] database and updated with the new chemical entities approved by the US FDA till July 2020.

4.2. Physicochemical Property Analysis. The physicochemical properties were calculated either using the DataWarrior program or RDKit[126] nodes implemented in KNIME platform 4.1.2.[127] GraphPad Prism was used for the computation of various statistical parameters (such as mean, median, 90th/10th percentiles, and confidence intervals) and hypothesis testing using the non-parametric one-way analysis of variance (Kruskal–Wallis method). The *p*-values were calculated at a 95% confidence level. DataWarrior was used to compute boxplots and associated *p*-values using the *t*-test and for calculating Spearman correlation coefficients. The frequency of rings for all categories of molecules was carried out by counting the "plain ring systems" using DataWarrior.

4.3. Data and Software Availability. The structures and related data of RAP molecules can be freely obtained from ChEMBL database (https://www.ebi.ac.uk/chembl/). The ASAM set of molecules was manually curated from the recent literature (Supporting Information, Table S1). The set of oral drugs was obtained from DrugCentral database, downloadable from https://drugcentral.org/download. The KNIME platform (v 4.1.2) is freely available at https://www.knime.com/downloads. The RDKit nodes for KNIME are available to download within the KNIME platform. The DataWarrior program (v 5.2.1) is an open-source cheminformatic software downloadable at http://www.openmolecules.org/datawarrior/download.html.

■ ASSOCIATED CONTENT

Supporting Information

The Supporting Information is available free of charge at https://pubs.acs.org/doi/10.1021/acsomega.1c00104.

Details of the ASAM category of molecules, distribution of low and high MW compounds, distribution of aromatic and aliphatic N-heterocycles, six most frequently occurring rings in each category, correlation between Actelion clog *P* versus the experimental log P and Actelion clog *P* versus StarDrop clog *P*, distribution of the mean of clog P, HBA, HBD, TPSA, #RB, #Ar, #CarboAr, #HetAr, #ArN, Fsp^3, and #BaN among low and high MW compounds within the IN, MA, HA, ASAM, and oral drugs categories, and statistical data (PDF)

■ AUTHOR INFORMATION

Corresponding Author

Sandeep Sundriyal − *Department of Pharmacy, Birla Institute of Technology and Science Pilani, Pilani, Rajasthan 333 031, India*; orcid.org/0000-0001-7823-8842; Email: sandeep.sundriyal@pilani.bits-pilani.ac.in

Author

Amritansh Bhanot − *Department of Pharmacy, Birla Institute of Technology and Science Pilani, Pilani, Rajasthan 333 031, India*

Complete contact information is available at: https://pubs.acs.org/10.1021/acsomega.1c00104

Notes

The authors declare no competing financial interest.

■ ACKNOWLEDGMENTS

The authors acknowledge the Department of Science and Technology, Science & Engineering Research Board (DST-SERB), New Delhi, for financial assistance through the Core Research Grant (CRG/2018/001527). We also thank Navya Bhandaru for assisting in the compilation of the library of oral drugs.

■ REFERENCES

(1) Wouters, O. J.; McKee, M.; Luyten, J. Estimated Research and Development Investment Needed to Bring a New Medicine to Market, 2009-2018. *JAMA, J. Am. Med. Assoc.* **2020**, *323*, 844−853.

(2) DiMasi, J. A.; Grabowski, H. G.; Hansen, R. W. Innovation in the Pharmaceutical Industry: New Estimates of R&D Costs. *J. Health Econ.* **2016**, *47*, 20−33.

(3) Dowden, H.; Munro, J. Trends in Clinical Success Rates and Therapeutic Focus. *Nat. Rev. Drug Discovery* **2019**, *18*, 495−496.

(4) Shultz, M. D. Two Decades under the Influence of the Rule of Five and the Changing Properties of Approved Oral Drugs. *J. Med. Chem.* **2019**, *62*, 1701−1714.

(5) Lipinski, C. A.; Lombardo, F.; Dominy, B. W.; Feeney, P. J. Experimental and Computational Approaches to Estimate Solubility and Permeability in Drug Discovery and Development Settings. *Adv. Drug Delivery Rev.* **1997**, *23*, 3−25.

(6) Petit, J.; Meurice, N.; Kaiser, C.; Maggiora, G. Softening the Rule of Five—Where to Draw the Line? *Bioorg. Med. Chem.* **2012**, *20*, 5343−5351.

(7) Abad-Zapatero, C. A Sorcerer's Apprentice and The Rule of Five: From Rule-of-Thumb to Commandment and Beyond. *Drug Discovery Today* **2007**, *12*, 995−997.

(8) Tinworth, C. P.; Young, R. J. Facts, Patterns, and Principles in Drug Discovery: Appraising the Rule of 5 with Measured Physicochemical Data. *J. Med. Chem.* **2020**, *63*, 10091−10108.

(9) Leeson, P. D. Molecular Inflation, Attrition and the Rule of Five. *Adv. Drug Delivery Rev.* **2016**, *101*, 22−33.

(10) Ritchie, T. J.; Macdonald, S. J. F. The Impact of Aromatic Ring Count on Compound Developability—Are Too Many Aromatic Rings a Liability in Drug Design? *Drug Discovery Today* **2009**, *14*, 1011−1020.

(11) Ritchie, T. J.; Macdonald, S. J. F.; Peace, S.; Pickett, S. D.; Luscombe, C. N. The Developability of Heteroaromatic and Heteroaliphatic Rings—Do Some Have a Better Pedigree as Potential Drug Molecules than Others? *MedChemComm* **2012**, *3*, 1062−1069.

(12) Ritchie, T. J.; MacDonald, S. J. F.; Young, R. J.; Pickett, S. D. The Impact of Aromatic Ring Count on Compound Developability: Further Insights by Examining Carbo- and Hetero-Aromatic and -Aliphatic Ring Types. *Drug Discovery Today* **2011**, *16*, 164−171.

(13) Lovering, F.; Bikker, J.; Humblet, C. Escape from Flatland: Increasing Saturation as an Approach to Improving Clinical Success. *J. Med. Chem.* **2009**, *52*, 6752−6756.

(14) Veber, D. F.; Johnson, S. R.; Cheng, H.-Y.; Smith, B. R.; Ward, K. W.; Kopple, K. D. Molecular Properties That Influence the Oral Bioavailability of Drug Candidates. *J. Med. Chem.* **2002**, *45*, 2615−2623.

(15) Whitty, A.; Zhong, M.; Viarengo, L.; Beglov, D.; Hall, D. R.; Vajda, S. Quantifying the Chameleonic Properties of Macrocycles and

Other High-Molecular-Weight Drugs. *Drug Discovery Today* **2016**, *21*, 712−717.
(16) Young, R. J.; Green, D. V. S.; Luscombe, C. N.; Hill, A. P. Getting Physical in Drug Discovery II: The Impact of Chromatographic Hydrophobicity Measurements and Aromaticity. *Drug Discovery Today* **2011**, *16*, 822−830.
(17) Degoey, D. A.; Chen, H.-J.; Cox, P. B.; Wendt, M. D. Beyond the Rule of 5: Lessons Learned from AbbVie's Drugs and Compound Collection. *J. Med. Chem.* **2018**, *61*, 2636−2651.
(18) Fullam, E.; Young, R. J. Physicochemical Properties and Mycobacterium Tuberculosis Transporters: Keys to Efficacious Antitubercular Drugs? *RSC Med. Chem.* **2021**, *12*, 45−56.
(19) Bickerton, G. R.; Paolini, G. V.; Besnard, J.; Muresan, S.; Hopkins, A. L. Quantifying the Chemical Beauty of Drugs. *Nat. Chem.* **2012**, *4*, 90−98.
(20) Young, R. J.; Leeson, P. D. Mapping the Efficiency and Physicochemical Trajectories of Successful Optimizations. *J. Med. Chem.* **2018**, *61*, 6421−6467.
(21) Leeson, P. D.; Springthorpe, B. The Influence of Drug-like Concepts on Decision-Making in Medicinal Chemistry. *Nat. Rev. Drug Discovery* **2007**, *6*, 881−890.
(22) Hopkins, A. L.; Groom, C. R.; Alex, A. Ligand Efficiency: A Useful Metric for Lead Selection. *Drug Discovery Today* **2004**, *9*, 430−431.
(23) Vieth, M.; Sutherland, J. J. Dependence of Molecular Properties on Proteomic Family for Marketed Oral Drugs. *J. Med. Chem.* **2006**, *49*, 3451−3453.
(24) Adrian, G.; Marcel, V.; Robert, B.; Richard, T. A Comparison of Physicochemical Property Profiles of Marketed Oral Drugs and Orally Bioavailable Anti-Cancer Protein Kinase Inhibitors in Clinical Development. *Curr. Top. Med. Chem.* **2007**, *7*, 1408−1422.
(25) Leeson, P. D.; Davis, A. M. Time-Related Differences in the Physical Property Profiles of Oral Drugs. *J. Med. Chem.* **2004**, *47*, 6338−6348.
(26) Gualtieri, M.; Baneres-Roquet, F.; Villain-Guillot, P.; Pugniere, M.; Leonetti, J.-P. The Antibiotics in the Chemical Space. *Curr. Med. Chem.* **2009**, *16*, 390−393.
(27) Macielag, M. J. Chemical Properties of Antimicrobials and Their Uniqueness. In *Antibiotic Discovery and Development*; Dougherty, T. J., Pucci, M. J., Eds.; Springer: New York, 2012; pp 793−820.
(28) Wager, T. T.; Chandrasekaran, R. Y.; Hou, X.; Troutman, M. D.; Verhoest, P. R.; Villalobos, A.; Will, Y. Defining Desirable Central Nervous System Drug Space through the Alignment of Molecular Properties, in Vitro ADME, and Safety Attributes. *ACS Chem. Neurosci.* **2010**, *1*, 420−434.
(29) Doan, K. M. M.; Humphreys, J. E.; Webster, L. O.; Wring, S. A.; Shampine, L. J.; Serabjit-Singh, C. J.; Adkison, K. K.; Polli, J. W. Passive Permeability and P-Glycoprotein-Mediated Efflux Differentiate Central Nervous System (CNS) and Non-CNS Marketed Drugs. *J. Pharmacol. Exp. Ther.* **2002**, *303*, 1029−1037.
(30) World Health Organization. WHO Malaria Report 2019. https://www.who.int/publications-detail/world-malaria-report-2019 (accessed Oct 23, 2020).
(31) Woodrow, C. J.; White, N. J. The Clinical Impact of Artemisinin Resistance in Southeast Asia and the Potential for Future Spread. *FEMS Microbiol. Rev.* **2017**, *41*, 34−48.
(32) Müller, O.; Lu, G. Y.; Von Seidlein, L. Geographic Expansion of Artemisinin Resistance. *J. Travel Med.* **2019**, *26*, taz030.
(33) Imwong, M.; Suwannasin, K.; Kunasol, C.; Sutawong, K.; Mayxay, M.; Rekol, H.; Smithuis, F. M.; Hlaing, T. M.; Tun, K. M.; van der Pluijm, R. W.; Tripura, R.; Miotto, O.; Menard, D.; Dhorda, M.; Day, N. P. J.; White, N. J.; Dondorp, A. M. The Spread of Artemisinin-Resistant Plasmodium Falciparum in the Greater Mekong Subregion: A Molecular Epidemiology Observational Study. *Lancet Infect. Dis.* **2017**, *17*, 491−497.
(34) Hassett, M. R.; Roepe, P. D. Origin and Spread of Evolving Artemisinin-Resistant Plasmodium Falciparum Malarial Parasites in Southeastc Asia. *Am. J. Trop. Med. Hyg.* **2019**, *101*, 1204−1211.
(35) Ashley, E. A.; Dhorda, M.; Fairhurst, R. M.; Amaratunga, C.; Lim, P.; Suon, S.; Sreng, S.; Anderson, J. M.; Mao, S.; Sam, B.; Sopha, C.; Chuor, C. M.; Nguon, C.; Sovannaroth, S.; Pukrittayakamee, S.; Jittamala, P.; Chotivanich, K.; Chutasmit, K.; Suchatsoonthorn, C.; Runcharoen, R.; Hien, T. T.; Thuy-Nhien, N. T.; Thanh, N. V.; Phu, N. H.; Htut, Y.; Han, K.-T.; Aye, K. H.; Mokuolu, O. A.; Olaosebikan, R. R.; Folaranmi, O. O.; Mayxay, M.; Khanthavong, M.; Hongvanthong, B.; Newton, P. N.; Onyamboko, M. A.; Fanello, C. I.; Tshefu, A. K.; Mishra, N.; Valecha, N.; Phyo, A. P.; Nosten, F.; Yi, P.; Tripura, R.; Borrmann, S.; Bashraheil, M.; Peshu, J.; Faiz, M. A.; Ghose, A.; Hossain, M. A.; Samad, R.; Rahman, M. R.; Hasan, M. M.; Islam, A.; Miotto, O.; Amato, R.; MacInnis, B.; Stalker, J.; Kwiatkowski, D. P.; Bozdech, Z.; Jeeyapant, A.; Cheah, P. Y.; Sakulthaew, T.; Chalk, J.; Intharabut, B.; Silamut, K.; Lee, S. J.; Vihokhern, B.; Kunasol, C.; Imwong, M.; Tarning, J.; Taylor, W. J.; Yeung, S.; Woodrow, C. J.; Flegg, J. A.; Das, D.; Smith, J.; Venkatesan, M.; Plowe, C. V.; Stepniewska, K.; Guerin, P. J.; Dondorp, A. M.; Day, N. P.; White, N. J. Spread of Artemisinin Resistance in Plasmodium Falciparum Malaria. *N. Engl. J. Med.* **2014**, *371*, 411−423.
(36) Conrad, M. D.; Rosenthal, P. J. Antimalarial Drug Resistance in Africa: The Calm before the Storm? *Lancet Infect. Dis.* **2019**, *19*, e338−e351.
(37) Ashley, E. A.; Phyo, A. P. Drugs in Development for Malaria. *Drugs* **2018**, *78*, 861−879.
(38) Tse, E. G.; Korsik, M.; Todd, M. H. The Past, Present and Future of Anti-Malarial Medicines. *Malar. J.* **2019**, *18*, 93.
(39) Okombo, J.; Chibale, K. Recent Updates in the Discovery and Development of Novel Antimalarial Drug Candidates. *MedChemComm* **2018**, *9*, 437−453.
(40) Burrows, J. N.; Duparc, S.; Gutteridge, W. E.; Hooft Van Huijsduijnen, R.; Kaszubska, W.; Macintyre, F.; Mazzuri, S.; Möhrle, J. J.; Wells, T. N. C. New Developments in Anti-Malarial Target Candidate and Product Profiles. *Malar. J.* **2017**, *16*, 26.
(41) Basore, K.; Cheng, Y.; Kushwaha, A. K.; Nguyen, S. T.; Desai, S. A. How Do Antimalarial Drugs Reach Their Intracellular Targets? *Front. Pharmacol.* **2015**, *6*, 91.
(42) Goldberg, D. E.; Zimmerberg, J. Hardly Vacuous: The Parasitophorous Vacuolar Membrane of Malaria Parasites. *Trends Parasitol.* **2020**, *36*, 138−146.
(43) Gamo, F.-J.; Sanz, L. M.; Vidal, J.; De Cozar, C.; Alvarez, E.; Lavandera, J.-L.; Vanderwall, D. E.; Green, D. V. S.; Kumar, V.; Hasan, S.; Brown, J. R.; Peishoff, C. E.; Cardon, L. R.; Garcia-Bustos, J. F. Thousands of Chemical Starting Points for Antimalarial Lead Identification. *Nature* **2010**, *465*, 305−310.
(44) Wenlock, M. C.; Austin, R. P.; Barton, P.; Davis, A. M.; Leeson, P. D. A Comparison of Physiochemical Property Profiles of Development and Marketed Oral Drugs. *J. Med. Chem.* **2003**, *46*, 1250−1256.
(45) Tyrchan, C.; Blomberg, N.; Engkvist, O.; Kogej, T.; Muresan, S. Physicochemical Property Profiles of Marketed Drugs, Clinical Candidates and Bioactive Compounds. *Bioorg. Med. Chem. Lett.* **2009**, *19*, 6943−6947.
(46) Bento, A. P.; Gaulton, A.; Hersey, A.; Bellis, L. J.; Chambers, J.; Davies, M.; Krüger, F. A.; Light, Y.; Mak, L.; McGlinchey, S.; Nowotka, M.; Papadatos, G.; Santos, R.; Overington, J. P. The ChEMBL Bioactivity Database: An Update. *Nucleic Acids Res.* **2014**, *42*, D1083−D1090.
(47) Gaulton, A.; Bellis, L. J.; Bento, A. P.; Chambers, J.; Davies, M.; Hersey, A.; Light, Y.; McGlinchey, S.; Michalovich, D.; Al-Lazikani, B.; Overington, J. P. ChEMBL: A Large-Scale Bioactivity Database for Drug Discovery. *Nucleic Acids Res.* **2012**, *40*, D1100−D1107.
(48) Ekins, S.; Williams, A. J. When Pharmaceutical Companies Publish Large Datasets: An Abundance of Riches or Fool's Gold? *Drug Discovery Today* **2010**, *15*, 812−815.
(49) Dimova, D.; Stumpfe, D.; Bajorath, J. Systematic Assessment of Coordinated Activity Cliffs Formed by Kinase Inhibitors and Detailed Characterization of Activity Cliff Clusters and Associated SAR Information. *Eur. J. Med. Chem.* **2015**, *90*, 414−427.

https://dx.doi.org/10.1021/acsomega.1c00104
ACS Omega 2021, 6, 6424−6437

(50) Ursu, O.; Holmes, J.; Bologa, C. G.; Yang, J. J.; Mathias, S. L.; Stathias, V.; Nguyen, D.-T.; Schürer, S.; Oprea, T. DrugCentral 2018: An Update. *Nucleic Acids Res.* **2019**, *47*, D963−D970.
(51) Pye, C. R.; Hewitt, W. M.; Schwochert, J.; Haddad, T. D.; Townsend, C. E.; Etienne, L.; Lao, Y.; Limberakis, C.; Furukawa, A.; Mathiowetz, A. M.; Price, D. A.; Liras, S.; Lokey, R. S. Nonclassical Size Dependence of Permeation Defines Bounds for Passive Adsorption of Large Drug Molecules. *J. Med. Chem.* **2017**, *60*, 1665−1672.
(52) Doak, B. C.; Over, B.; Giordanetto, F.; Kihlberg, J. Oral Druggable Space beyond the Rule of 5: Insights from Drugs and Clinical Candidates. *Chem. Biol.* **2014**, *21*, 1115−1142.
(53) Sander, T.; Freyss, J.; von Korff, M.; Rufener, C. DataWarrior: An Open-Source Program for Chemistry Aware Data Visualization and Analysis. *J. Chem. Inf. Model.* **2015**, *55*, 460−473.
(54) Mannhold, R.; Poda, G. I.; Ostermann, C.; Tetko, I. V. Calculation of Molecular Lipophilicity: State-of-the-Art and Comparison of Log P Methods on More than 96,000 Compounds. *J. Pharm. Sci.* **2009**, *98*, 861−893.
(55) Van de Waterbeemd, H.; Smith, D. A.; Beaumont, K.; Walker, D. K. Property-Based Design: Optimization of Drug Absorption and Pharmacokinetics. *J. Med. Chem.* **2001**, *44*, 1313−1333.
(56) Ertl, P.; Schuffenhauer, A. Estimation of Synthetic Accessibility Score of Drug-like Molecules Based on Molecular Complexity and Fragment Contributions. *J. Cheminf.* **2009**, *1*, 8.
(57) Egan, W. J.; Merz, K. M.; Baldwin, J. J. Prediction of Drug Absorption Using Multivariate Statistics. *J. Med. Chem.* **2000**, *43*, 3867−3877.
(58) Desai, S. A. Why Do Malaria Parasites Increase Host Erythrocyte Permeability? *Trends Parasitol.* **2014**, *30*, 151−159.
(59) Nguitragool, W.; Bokhari, A. A. B.; Pillai, A. D.; Rayavara, K.; Sharma, P.; Turpin, B.; Aravind, L.; Desai, S. A. Malaria Parasite Clag3 Genes Determine Channel-Mediated Nutrient Uptake by Infected Red Blood Cells. *Cell* **2011**, *145*, 665−677.
(60) Cohn, J. V.; Alkhalil, A.; Wagner, M. A.; Rajapandi, T.; Desai, S. A. Extracellular Lysines on the Plasmodial Surface Anion Channel Involved in Na+ Exclusion. *Mol. Biochem. Parasitol.* **2003**, *132*, 27−34.
(61) Desai, S. A.; Rosenberg, R. L. Pore Size of the Malaria Parasite's Nutrient Channel. *Proc. Natl. Acad. Sci. U.S.A.* **1997**, *94*, 2045−2049.
(62) Nyalwidhe, J.; Baumeister, S.; Hibbs, A. R.; Tawill, S.; Papakrivos, J.; Völker, U.; Lingelbach, K. A Nonpermeant Biotin Derivative Gains Access to the Parasitophorous Vacuole in Plasmodium Falciparum-Infected Erythrocytes Permeabilized with Streptolysin O. *J. Biol. Chem.* **2002**, *277*, 40005−40011.
(63) Desai, S. A.; Krogstad, D. J.; McCleskey, E. W. A Nutrient-Permeable Channel on the Intraerythrocytic Malaria Parasite. *Nature* **1993**, *362*, 643−646.
(64) Refsgaard, H. H. F.; Jensen, B. F.; Brockhoff, P. B.; Padkjær, S. B.; Guldbrandt, M.; Christensen, M. S. In Silico Prediction of Membrane Permeability from Calculated Molecular Parameters. *J. Med. Chem.* **2005**, *48*, 805−811.
(65) Hann, M. M. Molecular Obesity, Potency and Other Addictions in Drug Discovery. *MedChemComm* **2011**, *2*, 349−355.
(66) Schultes, S.; De Graaf, C.; Berger, H.; Mayer, M.; Steffen, A.; Haaksma, E. E. J.; De Esch, I. J. P.; Leurs, R.; Krämer, O. A Medicinal Chemistry Perspective on Melting Point: Matched Molecular Pair Analysis of the Effects of Simple Descriptors on the Melting Point of Drug-like Compounds. *MedChemComm* **2012**, *3*, 584−591.
(67) Withnall, M.; Chen, H.; Tetko, I. V. Matched Molecular Pair Analysis on Large Melting Point Datasets: A Big Data Perspective. *ChemMedChem* **2018**, *13*, 599−606.
(68) Ertl, P.; Rohde, B.; Selzer, P. Fast Calculation of Molecular Polar Surface Area as a Sum of Fragment-Based Contributions and Its Application to the Prediction of Drug Transport Properties. *J. Med. Chem.* **2000**, *43*, 3714−3717.
(69) Pennington, L. D.; Moustakas, D. T. The Necessary Nitrogen Atom: A Versatile High-Impact Design Element for Multiparameter Optimization. *J. Med. Chem.* **2017**, *60*, 3552−3579.
(70) Vitaku, E.; Smith, D. T.; Njardarson, J. T. Analysis of the Structural Diversity, Substitution Patterns, and Frequency of Nitrogen Heterocycles among U.S. FDA Approved Pharmaceuticals. *J. Med. Chem.* **2014**, *57*, 10257−10274.
(71) Kalaria, P. N.; Karad, S. C.; Raval, D. K. A Review on Diverse Heterocyclic Compounds as the Privileged Scaffolds in Antimalarial Drug Discovery. *Eur. J. Med. Chem.* **2018**, *158*, 917−936.
(72) Kaur, K.; Jain, M.; Reddy, R. P.; Jain, R. Quinolines and Structurally Related Heterocycles as Antimalarials. *Eur. J. Med. Chem.* **2010**, *45*, 3245−3264.
(73) Chugh, A.; Kumar, A.; Verma, A.; Kumar, S.; Kumar, P. A Review of Antimalarial Activity of Two or Three Nitrogen Atoms Containing Heterocyclic Compounds. *Med. Chem. Res.* **2020**, *29*, 1723−1750.
(74) Ertl, P.; Jelfs, S.; Mühlbacher, J.; Schuffenhauer, A.; Selzer, P. Quest for the Rings. In Silico Exploration of Ring Universe to Identify Novel Bioactive Heteroaromatic Scaffolds. *J. Med. Chem.* **2006**, *49*, 4568−4573.
(75) Parhizgar, A. R.; Tahghighi, A. Introducing New Antimalarial Analogues of Chloroquine and Amodiaquine: A Narrative Review. *Iran. J. Med. Sci.* **2017**, *42*, 115−128.
(76) Feng, L. S.; Xu, Z.; Chang, L.; Li, C.; Yan, X. F.; Gao, C.; Ding, C.; Zhao, F.; Shi, F.; Wu, X. Hybrid Molecules with Potential in Vitro Antiplasmodial and in Vivo Antimalarial Activity against Drug-Resistant Plasmodium Falciparum. *Med. Res. Rev.* **2020**, *40*, 931−971.
(77) Nqoro, X.; Tobeka, N.; Aderibigbe, B. Quinoline-Based Hybrid Compounds with Antimalarial Activity. *Molecules* **2017**, *22*, 2268.
(78) Vennerstrom, J. L.; Ellis, W. Y.; Ager, A. L.; Andersen, S. L.; Gerena, L.; Milhous, W. K. Bisquinolines. 1. N,N-Bis(7-Chloroquinolin-4-Yl)Alkanediamines with Potential against Chloroquine-Resistant Malaria. *J. Med. Chem.* **1992**, *35*, 2129−2134.
(79) Liebman, K. M.; Burgess, S. J.; Gunsaru, B.; Kelly, J. X.; Li, Y.; Morrill, W.; Liebman, M. C.; Peyton, D. H. Unsymmetrical Bisquinolines with High Potency against P. Falciparum Malaria. *Molecules* **2020**, *25*, 2251.
(80) Kondaparla, S.; Agarwal, P.; Srivastava, K.; Puri, S. K.; Katti, S. B. Design, Synthesis and in Vitro Antiplasmodial Activity of Some Bisquinolines against Chloroquine-Resistant Strain. *Chem. Biol. Drug Des.* **2017**, *89*, 901−906.
(81) Vennerstrom, J. L.; Ager, A. L.; Dorn, A.; Andersen, S. L.; Gerena, L.; Ridley, R. G.; Milhous, W. K. Bisquinolines. 2. Antimalarial N,N-Bis(7-Chloroquinolin-4- Yl)Heteroalkanediamines. *J. Med. Chem.* **1998**, *41*, 4360−4364.
(82) Egan, T. J. Haemozoin Formation. *Mol. Biochem. Parasitol.* **2008**, *157*, 127−136.
(83) Fong, K. Y.; Wright, D. W. Hemozoin and Antimalarial Drug Discovery. *Future Med. Chem.* **2013**, *5*, 1437−1450.
(84) Weissbuch, I.; Leiserowitz, L. Interplay between Malaria, Crystalline Hemozoin Formation, and Antimalarial Drug Action and Design. *Chem. Rev.* **2008**, *108*, 4899−4914.
(85) Combrinck, J. M.; Mabotha, T. E.; Ncokazi, K. K.; Ambele, M. A.; Taylor, D.; Smith, P. J.; Hoppe, H. C.; Egan, T. J. Insights into the Role of Heme in the Mechanism of Action of Antimalarials. *ACS Chem. Biol.* **2013**, *8*, 133−137.
(86) Olafson, K. N.; Nguyen, T. Q.; Rimer, J. D.; Vekilov, P. G. Antimalarials Inhibit Hematin Crystallization by Unique Drug−Surface Site Interactions. *Proc. Natl. Acad. Sci. U.S.A.* **2017**, *114*, 7531−7536.
(87) Sullivan, D. J. Quinolines Block Every Step of Malaria Heme Crystal Growth. *Proc. Natl. Acad. Sci. U.S.A.* **2017**, *114*, 7483−7485.
(88) Buller, R.; Peterson, M. L.; Almarsson, Ö.; Leiserowitz, L. Quinoline Binding Site on Malaria Pigment Crystal: A Rational Pathway for Antimalaria Drug Design. *Cryst. Growth Des.* **2002**, *2*, 553−562.
(89) Solomonov, I.; Osipova, M.; Feldman, Y.; Baehtz, C.; Kjaer, K.; Robinson, I. K.; Webster, G. T.; McNaughton, D.; Wood, B. R.; Weissbuch, I.; Leiserowitz, L. Crystal Nucleation, Growth, and Morphology of the Synthetic Malaria Pigment β-Hematin and the Effect Thereon by Quinoline Additives: The Malaria Pigment as a

https://dx.doi.org/10.1021/acsomega.1c00104
ACS Omega 2021, 6, 6424−6437

Target of Various Antimalarial Drugs. *J. Am. Chem. Soc.* **2007**, *129*, 2615−2627.
(90) Walloch, P.; Henke, B.; Häuer, S.; Bergmann, B.; Spielmann, T.; Beitz, E. Introduction of Scaffold Nitrogen Atoms Renders Inhibitors of the Malarial L-Lactate Transporter, PfFNT, Effective against the Gly107Ser Resistance Mutation. *J. Med. Chem.* **2020**, *63*, 9731−9741.
(91) Kappes, B.; Doerig, C. D.; Graeser, R. An Overview of Plasmodium Protein Kinases. *Parasitol. Today* **1999**, *15*, 449−454.
(92) Doerig, C.; Billker, O.; Haystead, T.; Sharma, P.; Tobin, A. B.; Waters, N. C. Protein Kinases of Malaria Parasites: An Update. *Trends Parasitol.* **2008**, *24*, 570−577.
(93) Cabrera, D. G.; Horatscheck, A.; Wilson, C. R.; Basarab, G.; Eyermann, C. J.; Chibale, K. Plasmodial Kinase Inhibitors: License to Cure? *J. Med. Chem.* **2018**, *61*, 8061−8077.
(94) Ward, S. E.; Beswick, P. What Does the Aromatic Ring Number Mean for Drug Design? *Expert Opin. Drug Discovery* **2014**, *9*, 995−1003.
(95) Thomas, V. H.; Bhattachar, S.; Hitchingham, L.; Zocharski, P.; Naath, M.; Surendran, N.; Stoner, C. L.; El-Kattan, A. The Road Map to Oral Bioavailability: An Industrial Perspective. *Expert Opin. Drug Metab. Toxicol.* **2006**, *2*, 591−608.
(96) Large, J. M.; Birchall, K.; Bouloc, N. S.; Merritt, A. T.; Smiljanic-Hurley, E.; Tsagris, D. J.; Wheldon, M. C.; Ansell, K. H.; Coombs, P. J.; Kettleborough, C. A.; Whalley, D.; Stewart, L. B.; Bowyer, P. W.; Baker, D. A.; Osborne, S. A. Potent Inhibitors of Malarial P. Falciparum Protein Kinase G: Improving the Cell Activity of a Series of Imidazopyridines. *Bioorg. Med. Chem. Lett.* **2019**, *29*, 509−514.
(97) Tsagris, D. J.; Birchall, K.; Bouloc, N.; Large, J. M.; Merritt, A.; Smiljanic-Hurley, E.; Wheldon, M.; Ansell, K. H.; Kettleborough, C.; Whalley, D.; Stewart, L. B.; Bowyer, P. W.; Baker, D. A.; Osborne, S. A. Trisubstituted Thiazoles as Potent and Selective Inhibitors of Plasmodium Falciparum Protein Kinase G (PfPKG). *Bioorg. Med. Chem. Lett.* **2018**, *28*, 3168−3173.
(98) Natarajan, J. K.; Alumasa, J. N.; Yearick, K.; Ekoue-Kovi, K. A.; Casabianca, L. B.; De Dios, A. C.; Wolf, C.; Roepe, P. D. 4-N-, 4-S-, and 4-O-Chloroquine Analogues: Influence of Side Chain Length and Quinolyl Nitrogen PKa on Activity vs Chloroquine Resistant Malaria. *J. Med. Chem.* **2008**, *51*, 3466−3479.
(99) Hameed P, S.; Solapure, S.; Patil, V.; Henrich, P. P.; Magistrado, P. A.; Bharath, S.; Murugan, K.; Viswanath, P.; Puttur, J.; Srivastava, A.; Bellale, E.; Panduga, V.; Shanbag, G.; Awasthy, D.; Landge, S.; Morayya, S.; Koushik, K.; Saralaya, R.; Raichurkar, A.; Rautela, N.; Roy Choudhury, N.; Ambady, A.; Nandishaiah, R.; Reddy, J.; Prabhakar, K. R.; Menasinakai, S.; Rudrapatna, S.; Chatterji, M.; Jiménez-Díaz, M. B.; Martínez, M. S.; Sanz, L. M.; Coburn-Flynn, O.; Fidock, D. A.; Lukens, A. K.; Wirth, D. F.; Bandodkar, B.; Mukherjee, K.; McLaughlin, R. E.; Waterson, D.; Rosenbrier-Ribeiro, L.; Hickling, K.; Balasubramanian, V.; Warner, P.; Hosagrahara, V.; Dudley, A.; Iyer, P. S.; Narayanan, S.; Kavanagh, S.; Sambandamurthy, V. K. Triaminopyrimidine Is a Fast-Killing and Long-Acting Antimalarial Clinical Candidate. *Nat. Commun.* **2015**, *6*, 6715.
(100) Masch, A.; Nasereddin, A.; Alder, A.; Bird, M. J.; Schweda, S. I.; Preu, L.; Doerig, C.; Dzikowski, R.; Gilberger, T. W.; Kunick, C. Structure-Activity Relationships in a Series of Antiplasmodial Thieno[2,3-b]Pyridines. *Malar. J.* **2019**, *18*, 89.
(101) Lavrado, J.; Cabal, G. G.; Prudêncio, M.; Mota, M. M.; Gut, J.; Rosenthal, P. J.; Díaz, C.; Guedes, R. C.; Dos Santos, D. J. V. A.; Bichenkova, E.; Douglas, K. T.; Moreira, R.; Paulo, A. Incorporation of Basic Side Chains into Cryptolepine Scaffold: Structure-Antimalarial Activity Relationships and Mechanistic Studies. *J. Med. Chem.* **2011**, *54*, 734−750.
(102) Egan, T. J.; Hunter, R.; Kaschula, C. H.; Marques, H. M.; Misplon, A.; Walden, J. Structure-Function Relationships in Amino-quinolines: Effect of Amino and Chloro Groups on Quinoline-Hematin Complex Formation, Inhibition of β-Hematin Formation, and Antiplasmodial Activity. *J. Med. Chem.* **2000**, *43*, 283−291.
(103) Tam, D. N. H.; Tawfik, G. M.; El-Qushayri, A. E.; Mehyar, G. M.; Istanbuly, S.; Karimzadeh, S.; Tu, V. L.; Tiwari, R.; Van Dat, T.; Nguyen, P. T. V.; Hirayama, K.; Huy, N. T. Correlation between Anti-Malarial and Anti-Haemozoin Activities of Anti-Malarial Compounds. *Malar. J.* **2020**, *19*, 298.
(104) Kaschula, C. H.; Egan, T. J.; Hunter, R.; Basilico, N.; Parapini, S.; Taramelli, D.; Pasini, E.; Monti, D. Structure−Activity Relationships in 4-Aminoquinoline Antiplasmodials. The Role of the Group at the 7-Position. *J. Med. Chem.* **2002**, *45*, 3531−3539.
(105) Yayon, A.; Cabantchik, Z. I.; Ginsburg, H. Identification of the Acidic Compartment of Plasmodium Falciparum-Infected Human Erythrocytes as the Target of the Antimalarial Drug Chloroquine. *EMBO J.* **1984**, *3*, 2695−2700.
(106) Kuhn, Y.; Rohrbach, P.; Lanzer, M. Quantitative PH Measurements in Plasmodium Falciparum-Infected Erythrocytes Using PHluorin. *Cell. Microbiol.* **2007**, *9*, 1004−1013.
(107) Bachhawat, K.; Thomas, C. J.; Surolia, N.; Surolia, A. Interaction of Chloroquine and Its Analogues with Heme: An Isothermal Titration Calorimetric Study. *Biochem. Biophys. Res. Commun.* **2000**, *276*, 1075−1079.
(108) O'Neill, P. M.; Posner, G. H. A Medicinal Chemistry Perspective on Artemisinin and Related Endoperoxides. *J. Med. Chem.* **2004**, *47*, 2945−2964.
(109) Teixeira, C.; Vale, N.; Pérez, B.; Gomes, A.; Gomes, J. R. B.; Gomes, P. "Recycling" Classical Drugs for Malaria. *Chem. Rev.* **2014**, *114*, 11164−11220.
(110) Chong, C. R.; Chen, X.; Shi, L.; Liu, J. O.; Sullivan, D. J. A Clinical Drug Library Screen Identifies Astemizole as an Antimalarial Agent. *Nat. Chem. Biol.* **2006**, *2*, 415−416.
(111) Da Cruz, F. P.; Martin, C.; Buchholz, K.; Lafuente-Monasterio, M. J.; Rodrigues, T.; Sönnichsen, B.; Moreira, R.; Gamo, F.-J.; Marti, M.; Mota, M. M.; Hannus, M.; Prudêncio, M. Drug Screen Targeted at Plasmodium Liver Stages Identifies a Potent Multistage Antimalarial Drug. *J. Infect. Dis.* **2012**, *205*, 1278−1286.
(112) Pazhayam, N. M.; Chhibber-Goel, J.; Sharma, A. New Leads for Drug Repurposing against Malaria. *Drug Discovery Today* **2019**, *24*, 263−271.
(113) Kaiser, M.; Mäser, P.; Tadoori, L. P.; Ioset, J. R.; Brun, R.; Sullivan, D. J. Antiprotozoal Activity Profiling of Approved Drugs: A Starting Point toward Drug Repositioning. *PLoS One* **2015**, *10*, No. e0135556.
(114) Gleeson, M. P.; Hersey, A.; Montanari, D.; Overington, J. Probing the Links between in Vitro Potency, ADMET and Physicochemical Parameters. *Nat. Rev. Drug Discovery* **2011**, *10*, 197−208.
(115) Martin, R. E. The Transportome of the Malaria Parasite. *Biol. Rev.* **2020**, *95*, 305−332.
(116) Cowell, A. N.; Istvan, E. S.; Lukens, A. K.; Gomez-Lorenzo, M. G.; Vanaerschot, M.; Sakata-Kato, T.; Flannery, E. L.; Magistrado, P.; Owen, E.; Abraham, M.; LaMonte, G.; Painter, H. J.; Williams, R. M.; Franco, V.; Linares, M.; Arriaga, I.; Bopp, S.; Corey, V. C.; Gnädig, N. F.; Coburn-Flynn, O.; Reimer, C.; Gupta, P.; Murithi, J. M.; Moura, P. A.; Fuchs, O.; Sasaki, E.; Kim, S. W.; Teng, C. H.; Wang, L. T.; Akidil, A.; Adjalley, S.; Willis, P. A.; Siegel, D.; Tanaseichuk, O.; Zhong, Y.; Zhou, Y.; Llinás, M.; Ottilie, S.; Gamo, F.-J.; Lee, M. C. S.; Goldberg, D. E.; Fidock, D. A.; Wirth, D. F.; Winzeler, E. A. Mapping the Malaria Parasite Druggable Genome by Using in Vitro Evolution and Chemogenomics. *Science* **2018**, *359*, 191−199.
(117) Meier, A.; Erler, H.; Beitz, E. Targeting Channels and Transporters in Protozoan Parasite Infections. *Front. Chem.* **2018**, *6*, 88.
(118) Dobson, P. D.; Kell, D. B. Carrier-Mediated Cellular Uptake of Pharmaceutical Drugs: An Exception or the Rule? *Nat. Rev. Drug Discovery* **2008**, *7*, 205−220.
(119) Kell, D. B. What Would Be the Observable Consequences If Phospholipid Bilayer Diffusion of Drugs into Cells Is Negligible? *Trends Pharmacol. Sci.* **2015**, *36*, 15−21.

https://dx.doi.org/10.1021/acsomega.1c00104
ACS Omega 2021, 6, 6424−6437

(120) Kell, D. B.; Oliver, S. G. How Drugs Get into Cells: Tested and Testable Predictions to Help Discriminate between Transporter-Mediated Uptake and Lipoidal Bilayer Diffusion. *Front. Pharmacol.* **2014**, *5*, 231.
(121) Kell, D. B.; Dobson, P. D.; Oliver, S. G. Pharmaceutical Drug Transport: The Issues and the Implications That It Is Essentially Carrier-Mediated Only. *Drug Discovery Today* **2011**, *16*, 704−714.
(122) O'Hagan, S.; Swainston, N.; Handl, J.; Kell, D. B. A 'Rule of 0.5' for the Metabolite-Likeness of Approved Pharmaceutical Drugs. *Metabolomics* **2015**, *11*, 323−339.
(123) Charman, S. A.; Andreu, A.; Barker, H.; Blundell, S.; Campbell, A.; Campbell, M.; Chen, G.; Chiu, F. C. K.; Crighton, E.; Katneni, K.; Morizzi, J.; Patil, R.; Pham, T.; Ryan, E.; Saunders, J.; Shackleford, D. M.; White, K. L.; Almond, L.; Dickins, M.; Smith, D. A.; Moehrle, J. J.; Burrows, J. N.; Abla, N. An in Vitro Toolbox to Accelerate Anti-Malarial Drug Discovery and Development. *Malar. J.* **2020**, *19*, 1.
(124) CHEMBL26, release date March 2020; 10.6019/CHEMBL.database.26.
(125) GSK-TCAMS Dataset. https://chembl.gitbook.io/chembl-ntd/downloads/deposited-set-1-gsk-tcams-dataset-20th-may-2010 (accessed Oct 3, 2020).
(126) Landrum, G.; et al. RDKit: Open-Source Cheminformatics. 2006, http://www.rdkit.org (accessed on September 1, 2020).
(127) Berthold, M. R.; Cebron, N.; Dill, F.; Gabriel, T. R.; Kötter, T.; Meinl, T.; Ohl, P.; Sieb, C.; Thiel, K.; Wiswedel, B. KNIME: The Konstanz Information Miner. *Studies in Classification, Data Analysis, and Knowledge Organization (GfKL 2007)*; Springer, 2007.

https://dx.doi.org/10.1021/acsomega.1c00104
ACS Omega 2021, 6, 6424−6437